Effect of Adhesive Interactions on Static Friction at the Atomic Scale

Carolyn J. Carkner, Sarah M. Haw, and Nicholas J. Mosey*

Department of Chemistry, Queen's University, Kingston, ON, Canada K7L 3N6

(Received 14 May 2010; published 30 July 2010)

First-principles molecular dynamics (FPMD) simulations were used to study static friction, F_s, using model systems based on bulk and hydroxylated forms of Al_2O_3. The results demonstrate that F_s is significantly affected by adhesive interactions and by changes in the numbers of those interactions through the formation and dissociation of bonds across the slip interface. A model that directly incorporates the strengths of the adhesive interactions during slip is introduced to account for the effects on F_s and is found to perform satisfactorily. A procedure is developed to evaluate the strengths of these interactions using first-principles calculations. As a whole, the work clarifies how adhesive interactions affect F_s, provides a means of reducing the number of fit parameters used in modeling friction, and illustrates the importance of accounting for changes in bonding during simulations of friction.

DOI: 10.1103/PhysRevLett.105.056102 PACS numbers: 68.35.Af, 83.10.Gr, 83.10.Rs

Friction is a ubiquitous phenomenon of fundamental and practical interest, relating to topics ranging from the atomic-level interactions in interfaces to energy losses in devices containing sliding surfaces. This broad importance has driven research into friction for centuries. Early studies [1] led to the central concept that the tangential force required to slide an object along a surface (called the friction force, F) is proportional to the load, L, applied normal to that surface. This relationship is summarized as $F = \mu L$, where μ is the coefficient of friction. This equation indicates that $F = 0$ when $L = 0$ and that F should not depend on the area of the contact, A. These observations are commonly termed Amontons's laws.

Modern studies show that Amontons's laws are violated if adhesive interactions exist between the surfaces forming the contact [2]. This insight has been obtained through experimental studies of friction on small length scales [3,4], as well as molecular dynamics simulations [5,6]. These deviations are not apparent at large length scales because there are few asperities in contact and the number of adhesive interactions per unit area is small. However, understanding the effects of adhesion on friction in devices with inherently small length scales is of basic interest and can aid in miniaturization efforts, with friction being a major impediment to developing practical nano- and micro-electromechanical systems [7].

Friction in the presence of adhesive interactions is often described by two-term models [8–10]:

$$F = C_1 A + C_2 L \tag{1}$$

where C_1 and C_2 are constants. Equations of this form can accurately reproduce experimental values of F by treating C_1 and C_2 as fitted parameters. It would be beneficial, however, to have a means of evaluating these parameters *a priori* so they can be used as input into friction models, instead of being treated as fitted quantities. To do this, it is necessary to understand the meaning of these parameters, and to develop ways to calculate them using basic properties of the system.

Herein, we use first-principles molecular dynamics (FPMD) simulations to study static friction under adhesive conditions in sliding contacts composed of bulk and hydroxylated forms of alumina (Al_2O_3). The use of methods that explicitly treat the electronic structure (ES) is a departure from conventional simulations of friction [5,6], which employ force fields or coarse-grained models, yet provides a more accurate description of adhesive interactions and changes in those interactions through bond formation and dissociation. The results demonstrate that the static friction force, F_s, can be modeled accurately using a form of Eq. (1) in which C_1 is the sum of the forces required to rupture the bonds across the interface during slip, clarifying the nature of C_1. A method is proposed for evaluating the rupture forces, providing a practical means of obtaining C_1 without fitting to experimental data.

The calculations were performed using the models in Fig. 1. Figure 1(a) corresponds to bulk Al_2O_3. The structure in Fig. 1(b) was formed by cleaving Al_2O_3 to yield two Al-terminated (0001) surfaces, adding a hydroxyl group to each terminal Al^{3+} ion and a proton to the next subsurface oxygen along $[10\bar{1}0]$ and is designated "hydrox-LP." The structure in Fig. 1(c) was observed when hydrox-LP was exposed to $L > 3.2$ nN, causing the hydroxyl groups on either side of the interface to interdigitate and leading to proton transfer across the interface. This structure is designated "hydrox-HP." All models were based on a $2 \times 2 \times 1$ representation of the hexagonal unit cells and were treated with 3D periodic boundary conditions.

FPMD simulations were performed within the Car-Parrinello formalism [11] using a version of the Quantum-Espresso package that we modified to apply predefined strain rates [12]. The ES was evaluated with density functional theory [13] using the exchange-correlation functional of Perdew, Burke, and Ernzerhof [14]. The valence states were represented as plane waves

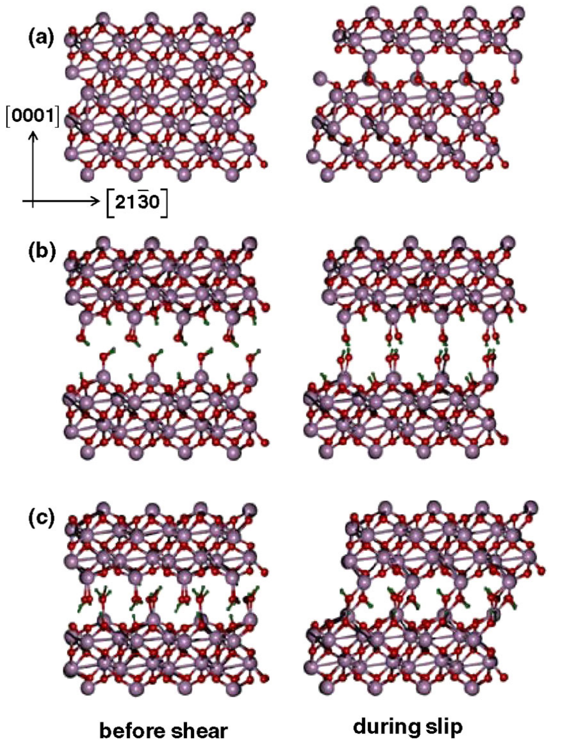

FIG. 1 (color online). Structures from the simulations before shear strain has been applied and during slip. (a) Bulk Al_2O_3 at $L = 0$ nN. (b) Hydrox-LP at $L = 0$ nN. (c) Hydrox-HP at $L = 8$ nN. The models shown have been repeated twice along the vectors defining the slip plane. Al, O, and H atoms are represented by large purple, small red, and smaller green spheres, respectively.

expanded at the Γ point to a kinetic energy cutoff of 30 Ry and the core states were represented by ultrasoft pseudopotentials [15]. The constant cutoff approach of Bernasconi *et al.* [16] was used throughout. Tests showed that this methodology accurately reproduces previously reported experimental and calculated data regarding the crystal structure (this work: $|\mathbf{a}| = 4.792$ Å, $|\mathbf{c}| = 13.071$ Å; experiment [17]: $|\mathbf{a}| = 4.759$ Å, $|\mathbf{c}| = 12.991$ Å), $(0001) - Al_2O_3$ surface energy (this work: $\gamma = 1.58\ \mathrm{J/m^2}$; previous calculation [18]: $\gamma = 1.49\ \mathrm{J/m^2}$), dissociation energy of H_2O on (0001)-Al_2O_3 (this work: 1.38 eV; previous calculation [19]: 1.44 eV) and Young's modulus (this work: $G = 402$ GPa; experiment [20]: $G = 345$ to 409 GPa). The dynamics were performed using a time step of 0.121 fs and an orbital mass of 400.0 au. The systems were equilibrated at 300 K using Nose-Hoover thermostats [21,22]. Temperature controls were removed after equilibration and the systems were sheared.

F_s values were obtained by performing simulations in which the system was sheared along $[21\bar{3}0]$ by altering the x and y components of $\mathbf{c}$ such that the top of the simulation cell moved along this direction at a rate of 1.0 Å/ps. This direction was selected based on experiments indicating this is the preferred basal slip direction in bulk Al_2O_3 [23] and potential energy scans on the (0001) plane of bulk Al_2O_3. Different values of L were maintained by allowing the height of the cell to vary according to an effectively one-dimensional version of Parrinello-Rahman dynamics [24]. The lateral lattice vectors were kept constant. Events corresponding to the onset of slip were identified in all simulations. The tangential force along the slip direction at these points was taken as F_s.

The F_s values are plotted in Fig. 2. The bulk and hydrox-LP systems exhibit linear relationships between F_s and L. The F_s values for these two systems deviate from Amontons's laws, with $F_s = 16.5$ and 1.8 nN when $L = 0$ nN for the bulk and hydrox-LP systems, respectively. The F_s values for these two systems can be accurately represented by Eq. (1), with least-squares fits of the data providing C_1A and C_2. The fitted and FPMD F_s values were in good agreement with mean absolute errors (MAEs) of 0.3 and 0.0 nN and mean absolute percent errors (MAPEs) of 1.6 and 0.8% for the bulk and hydrox-LP systems, respectively. This agreement is evident from the comparison of the FPMD and predicted values in Fig. 3 (solid symbols).

The data in Fig. 2 for the hydrox-HP system are not represented accurately using a linear relationship between F_s and L as in Eq. (1), with MAPE = 26.5%. This is because Al-O bonds formed across the interface between the initiation of shear and onset of slip, as shown in Fig. 1. The number of Al-O bonds, $n_{\text{Al-O}}$, that formed at different L are given in Fig. 2. Clearly, $n_{\text{Al-O}}$ does not correlate with L, which is due to the dependence of bond formation on the instantaneous structure and dynamics of the system, which vary between simulations. The effects of bond formation on F_s can by described by extending Eq. (1) to include changes in the number of Al-O bonds as:

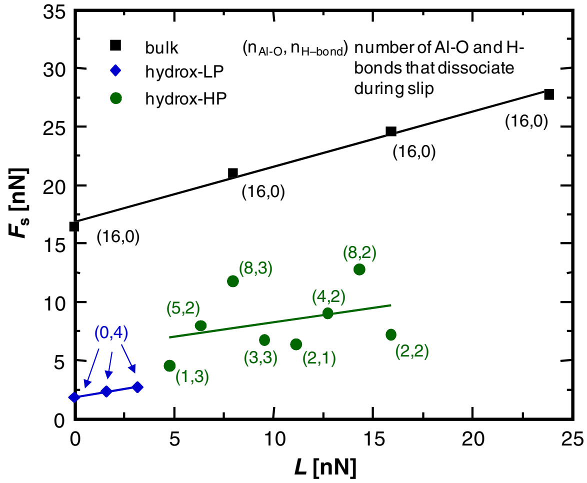

FIG. 2 (color online). F_s as a function of L for the bulk, hydrox-LP and hydrox-HP systems. The lines designate linear least-square fits of the calculated data. The number of Al-O and hydrogen bonds that dissociated during the slip events are shown in brackets at each L.

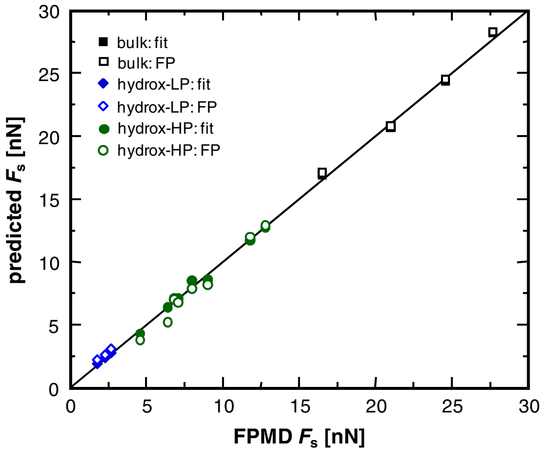

FIG. 3 (color online). Comparison between the FPMD values of F_s and those predicted with Eq. (2) using the parameters obtained through least-squares fitting (solid symbols) and with Eq. (3) using f_i obtained through first-principles (FP) calculations (open symbols). The solid line corresponds to perfect agreement between the predicted and FPMD values. Note that the solid squares lie almost entirely below the open squares.

$$F_s = C_1A + C_2L + C_3N_{\text{Al-O}}A \qquad (2)$$

where C_3 is a constant with units of force and $N_{\text{Al}-\text{O}}$ is the number of bonds formed prior to slip per unit area, i.e., $n_{\text{Al}-\text{O}} = N_{\text{Al}-\text{O}}A$. C_1, C_2, and C_3 were obtained by fitting the F_s values for hydrox-HP to Eq. (2). The F_s values obtained with the fitted parameters were in very good agreement with the FPMD values, with MAE = 0.209 nN and MAPE = 2.8%. This agreement is clear from Fig. 3 (solid circles). Note that Eq. (2) reduces to Eq. (1) when $N = 0$, and can be used when no new bonds form prior to slip.

The results demonstrate that Eq. (2) can account for deviations from Amontons's laws due to adhesive interactions, including cases where these interactions change during slip. In what follows, we investigate the nature of C_1 and C_3 and devise a strategy for calculating these quantities from first principles. Such capabilities may be useful in predictive modeling of friction coefficients.

Derjaguin suggested that $C_1 = \mu P_0$, where P_0 is a pressure acting normal to the slip plane due to adhesive interactions [9]. Defining $L_0 = P_0A$, this assumption is equivalent to $F_s = \mu(L_0 + L)$. It is reasonable to equate P_0 with the tensile strength, σ_c, of the interface, since this is the stress required to overcome the adhesive interactions. $\sigma_c = 36.9$ and 2.6 GPa ($L_0 = 29.3$ and 2.1 nN) were evaluated for the bulk and hydrox-LP systems, respectively, using methods described previously [25]. Using these values of L_0 to fit the FPMD values of F_s to $F_s = \mu(L_0 + L)$ yields $F_s = 3.0$ and 1.3 nN when $L_0 + L = 0$ for the bulk and hydrox-LP systems, respectively. If the assumption that $C_1 = \mu P_0$ was correct, both F_s values would be zero. An alternate definition of $C_1 = P_0 = \sigma_c$, yielding $F_s = L_0 + \mu L$, also performs poorly when applied to the bulk system (MAPE = 58.0%), yet reproduces the data for hydrox-LP to a reasonable level of agreement (MAPE = 10.2%). These results suggest that C_1 should not be associated with P_0.

C_1 has also been associated previously with an intrinsic shear strength, τ_c [8,10]. We suggest that $C_1 = \tau_c = \sum_{i=1}^{n_{\text{ad}}} f_iN_i$ where i runs over the different types of bonds, f_i is the force required to dissociate a bond of type i during slip, and N_i is the number of bonds of type i per unit area. Recognizing that the third term on the RHS of Eq. (2) corresponds to adhesive interactions, and hence $C_3 = f_{\text{Al-O}}$, the first and third terms on the RHS of Eq. (2) can be combined, yielding:

$$F_s = A\sum_{i=1}^{n_{\text{ad}}} f_iN_i + C_2L. \qquad (3)$$

This equation accounts for deviations from Amontons's laws with adhesive interactions, i.e., F_s is area dependent and nonzero at $L = 0$, and recovers $F_s = \mu L$ without adhesive interactions. The formulation of the first term on the RHS of Eq. (3) in terms of fundamental quantities reduces the number of fitted parameters needed to model F_s in the presence of adhesive interactions. The remaining fitted parameter, C_2, incorporates μ and it is not clear based on the results how to express this quantity in terms of fundamental quantities; although suggestions have been proposed previously [8,10].

To interpret experimental data, where one cannot observe and count bonds forming and dissociating during slip, the values of N_i that enter into Eq. (3) can be estimated with statistical methods for estimating the number of bonds present during sliding, such as the Weibull distribution [2,26]. The following procedure can be used to obtain f_i from ES calculations of well-defined models of the interface. First, σ_c is evaluated along the direction normal to the slip plane, and converted to a load, $L_c = \sigma_cA$. This load is due to the forces required to break all bonds across the interface. Each bond, j, has an intrinsic rupture force, f_j^0, corresponding to the force required to break the bond through elongation, and forms an angle, θ_j, to the surface normal. Assuming that the contribution of each bond to L_c is given by the projection of f_j^0 along the surface normal yields $L_c = \sum_j f_j^0 \cos(\theta_j)$, where j runs over all bonds broken when fracture occurs. Assuming that all bonds of a given type have the same f_j^0, this expression can be used to evaluate f_j^0 in systems where only one type of bond spans the interface if L_c and all values of θ_j are known. Once f_j^0 is known, it can be projected into the slip plane as $f_j^p = f_j^0 \sin(\theta_j)$. Each projection will form an angle, ϕ_j, with the slip direction, and the force required to rupture bond j during slip is given by $f_j^s = f_j^p \cos(\phi_j) = f_j^0 \sin(\theta_j)\cos(\theta_j)$. f_i is then taken as the average of the f_j^s values for all bonds that dissociate during slip. Similar practices have been used successfully to relate properties such as hardness to the structure of materials [27]. Of course, experiments are not typically performed with the atomically smooth surfaces employed in the calculations, and factors such as surface roughness may affect the accuracy of this projection method when applied to real systems.

The process described above was applied to the bulk and hydrox-LP systems, yielding $f_i = 1.07$ and 0.54 nN for the Al-O and hydrogen bonds, respectively. These values were used with the number of bonds that dissociated during slip to evaluate the first term on the RHS of Eq. (3) for the bulk, hydrox-LP and hydrox-HP systems. F_s values were then predicted by fitting the FPMD F_s values to Eq. (3), treating C_2 as a fit parameter. The results are presented in Fig. 3 as open symbols and show that using Eq. (3) with f_i obtained from the ES calculations accurately reproduces the FPMD values of F_s. Quantitatively, MAE $= 0.3$, 0.3, and 0.4 nN and MAPE $= 1.6\%$, 13.7% and 6.7% were obtained for the bulk, hydrox-LP, and hydrox-HP systems, respectively. The good agreement validates Eq. (3) and the assertion that $C_1 = \tau_c = \sum_{i=1}^{n_{\mathrm{ad}}} f_i N_i$, clarifying the nature of C_1. The good performance for hydrox-HP is remarkable because f_i were not obtained through calculations on this system, indicating a degree of transferability in these values.

Overall, the results demonstrate that F_s can be modeled accurately with Eq. (3) even in the presence of adhesive interactions. The results show that adhesive interactions introduce an effective shear strength, $\tau_c = \sum_{i=1}^{n_{\mathrm{ad}}} f_i N_i$, which must be overcome for sliding to occur even when $L = 0$. This interpretation clarifies the physical origin of deviations from Amontons's laws in the presence of adhesive interactions, leading to F_s that is area dependent and nonzero when $L = 0$. The ability to evaluate f_i with ES calculations has the benefit of reducing the number of parameters that must be fit when predicting friction coefficients from experimental data. From a methodological standpoint, the study illustrates that the use of FPMD simulations can provide important atomic-level insight into the effects of changes in chemical bonding on F_s. Such changes in bonding cannot be described accurately without the use of these methods that explicitly consider the ES. Although beyond the scope of the present study, it is likely that the presented model could be applied to kinetic friction by incorporating a scaling factor that accounts for the effective reduction in the bond rupture forces when thermal energy is available under sliding conditions. An additional avenue worth further investigation is the area dependence, with the present atomic-level study suggesting that $F_s \propto A$ for constant L and theories based on contact mechanics proposing $F_s \propto L/\sqrt{A}$ [3].

We thank Dr. Hongjuan Zhu for discussions regarding the manuscript. Financial support from the Natural Sciences and Engineering Research Council (NSERC) of Canada and the Ontario Ministry of Research and Innovation is gratefully acknowledged. Computing resources were provided by the Shared Hierarchical Academic Research Computing Network (SHARCNET) and the Résaue Québécois de Calcul de Haute Performance (RQCHP).

---

*nicholas.mosey@chem.queensu.ca

[1] G. Amontons, Memoires de l'Academie Royale A 257 (1699).
[2] J. Gao, W.D. Luedtke, D. Gourdon, M. Ruth, J.N. Israelachvili, and U. Landman, J. Phys. Chem. B **108**, 3410 (2004).
[3] A. Schirmeisen and U.D. Schwarz, Chem. Phys. Chem. **10**, 2373 (2009).
[4] H. Holscher, A. Schirmeisen, and U.D. Schwarz, Phil. Trans. R. Soc. A **366**, 1383 (2008).
[5] J.A. Harrison, G. Gao, J.D. Schall, M.T. Knippenberg, and P.T. Mikulski, Phil. Trans. R. Soc. A **366**, 1469 (2008).
[6] N.J. Mosey and M.H. Muser, in *Reviews in Computational Chemistry*, edited by K.B. Lipkowitz, R. Larter, and T.R. Cundari (Wiley-VCH, New York, 2007).
[7] K.S. Breuer, in *MEMS: Introduction and Fundamentals*, edited by M. Gad-el-Hak (CRC/Taylor & Francis, Boca Raton, FL, 2006).
[8] J.N. Israelachvili and A.D. Berman, in *Handbook of Micro/Nanotribology*, edited by B. Bhushan (CRC Press, Boca Raton, FL, 1999).
[9] B.V. Derjaguin, Wear **128**, 19 (1988).
[10] B.J. Briscoe and D.C. Evans, Proc. R. Soc. A **380**, 389 (1982).
[11] R. Car and M. Parrinello, Phys. Rev. Lett. **55**, 2471 (1985).
[12] P. Giannozzi, S. Baroni, and N. Bonini *et al.*, J. Phys. Condens. Matter **21**, 395502 (2009).
[13] W. Kohn and L.J. Sham, Phys. Rev. **140**, A1133 (1965).
[14] J.P. Perdew, K. Burke, and M. Ernzerhof, Phys. Rev. Lett. **77**, 3865 (1996).
[15] D. Vanderbilt, Phys. Rev. B **41**, 7892 (1990).
[16] M. Bernasconi, G.L. Chiarotti, P. Focher, S. Scandolo, E. Tosatti, and M. Parrinello, J. Phys. Chem. Solids **56**, 501 (1995).
[17] R.E. Newnham and Y.M. de Haan, Z. Kristallogr. **117**, 235 (1962).
[18] R.L. Hayes, M. Ortiz, and E.A. Carter, Phys. Rev. B **69**, 172104 (2004).
[19] K.C. Hass, W.F. Schneider, A. Curioni, and W. Andreoni, J. Phys. Chem. B **104**, 5527 (2000).
[20] J.R. Shackelford and W. Alexander, *Materials Science and Engineering Handbook* (CRC Press, Boca Raton, FL, 2001).
[21] W.G. Hoover, Phys. Rev. A **31**, 1695 (1985).
[22] S. Nose, J. Chem. Phys. **81**, 511 (1984).
[23] A.H. Heuer, K.P.D. Lagerlof, and J. Castaing, Philos. Mag. A **78**, 747 (1998).
[24] M. Parrinello and A. Rahman, Phys. Rev. Lett. **45**, 1196 (1980).
[25] N.J. Mosey and E.A. Carter, J. Mech. Phys. Solids **57**, 287 (2009).
[26] W. Weibull, J. Appl. Mech. **18**, 293 (1951).
[27] A. Simunek, Phys. Rev. B **80**, 060103 (2009).